



# Diffusion coefficient of $\text{Li}^+$ in solid-state rechargeable battery materials

A.A. Andriiko<sup>\*</sup>, P.V. Rudenok, L.I. Nyrkova

*Institute of General and Inorganic Chemistry, 32 / 34 Prospect Palladina, Kiev 252142, Ukraine*

Received 2 May 1997; revised 9 July 1997

---

## Abstract

Simple mathematical model of charge/discharge process was developed, and the method of  $\text{Li}^+$  diffusion coefficient determination was elaborated based on the analysis of galvanostatic curves. The model and the method also enable the theoretical capacity of the rechargeable material to be found. © 1998 Elsevier Science S.A.

*Keywords:* Lithium ions; Intercalation; Diffusion; Rechargeable electrodes

---

## 1. Introduction

Presently, a number of researches on lithium batteries are devoted to the development of solid materials capable of reversible electrochemical lithium intercalation. In particular, concerning the positive electrode, several compounds with acceptable values of reversible capacities, voltages and cyclabilities have been proposed. Among them, the layered oxides  $\text{LiCoO}_2$  and  $\text{LiNiO}_2$  [1,2] and spinel-structured  $\text{LiMn}_2\text{O}_4$  [3,4] are regarded as most promising. These materials operate at rather high, significantly above 4 V vs. Li, working potentials, which may cause the oxidation of common organic electrolytes and thus, increase self-discharge. From this point of view, the materials operating at  $\sim 3$  V vs. Li, e.g., newly developed oxides of  $\text{Li}_2\text{O}-\text{MnO}_2$  series [5], could be preferable.

The development of commercial rechargeable Li batteries with solid electrodes demands the rates of electrochemical Li insertion to be known, in order to determine such important characteristics as charge regimes (current and time). As far as the rate of intercalation/deintercalation are limited by  $\text{Li}^+$  ion diffusion, the  $\text{Li}^+$  diffusion coefficient value, along with the geometric size (thickness), is eventually responsible for these parameters. In this paper we present a simple mathematic model that permits calculation of the  $\text{Li}^+$  diffusion coefficient from the galvanostatic experiments.

## 2. The model of galvanostatic charge/discharge

The electrochemical insertion of  $\text{Li}^+$  in solid material (and the reverse process) is represented as filling of the ‘vacancies’, that is, the sites that exist in bulk material and can be occupied (or quitted) by Li:



the electrons being commonly supplied by conductive matrix formed with the addition of fine graphite particles.

If the process (Eq. (1)) is governed by  $\text{Li}^+$  diffusion, then the concentration of Li (or free vacancies) varies in time in accordance with the second Fick’s differential equation:

$$\frac{\partial C}{\partial t} = D \cdot \frac{\partial^2 C}{\partial x^2}, \quad (2)$$

with initial condition

$$t = 0; C = C_0. \quad (3)$$

Since the one-dimensional diffusion in the layer of thickness  $l$  is considered under the galvanostatic regime, then the boundary condition at the plane  $x = 0$  (at current collector) is

$$D \cdot \frac{\partial C}{\partial x} \Big|_{x=0} = \frac{i}{F}, \quad (4)$$

where  $i$  = current density,  $F$  = Faraday constant.

The second boundary condition can be written in the form of integral equation of material balance:

$$\int_0^l C dx = C_0 \cdot l - i \cdot t / F. \quad (5)$$

---

<sup>\*</sup> Corresponding author. Ukrainian Natl. Acad. Sci., V.I. Vernadskii Institute of General and Inorganic Chemistry, 32/34 Palladin Prospect, 252680 Kiev-142, Ukraine.

Eq. (2), with initial and boundary conditions (Eqs. (3)–(5)), describes the galvanostatic intercalation of  $\text{Li}^+$  ions in assumptions that, first, the rate of electrochemical reaction is high relatively to the rate of transport and, secondly, the diffusion coefficient is independent on the concentration of occupied sites.

From solution of Eqs. (2)–(5), the dependence of the achieved capacity on the current density can be obtained in the form:

$$i \cdot \tau = f(i), \quad (6)$$

where  $\tau$  is the time, when the process is finished. We determine it as the time when zero concentration of free vacancies (discharge) or  $\text{Li}^+$  (charge) is achieved at the plane  $x = 0$ :

$$C(\tau)|_{x=0} = 0. \quad (7)$$

It was obtained for two limiting cases (see Appendix A).

### 2.1. Thick layers, large currents

$$\frac{D \cdot \tau}{l^2} \ll 1. \quad (8)$$

The solution in this case takes the familiar form of Sand's equation for transition time in chronopotentiometry:

$$i \cdot \sqrt{\tau} = \frac{1}{2} \cdot \sqrt{\pi \cdot D} \cdot F \cdot C_0 \quad (9)$$

or

$$i \cdot \tau = \pi \cdot D \cdot F^2 \cdot C_0^2 / 4 \cdot i. \quad (10)$$

Thus, the achieved capacity under the condition (Eq. (8)) varies inversely with current.

### 2.2. Thin layers, small currents

$$\frac{D \cdot \tau}{l^2} \gg 1. \quad (11)$$

The dependence (Eq. 6) takes the form

$$i \cdot \tau = l \cdot F \cdot C_0 - (l^2 / 3 \cdot D) i. \quad (12)$$

In this case, the achieved capacity increases linearly with the decrease of the current, and tends to theoretical capacity at  $i \rightarrow 0$ .

## 3. Experimental

The experimental verification of equations obtained was carried out using the prepared earlier oxides  $\text{Li}_2\text{O}-\text{MnO}_2$  [5] in button cells of 2325 size. The negative electrode was made of Li–Al alloy, and 1 M solution of  $\text{LiClO}_4$  in propylenecarbonate was used as electrolyte.

The positive electrode was prepared as follows.

The paste contained 25 mass % of graphite powder, 50 of teflon binder and 25 of acetylene black was rolled to form 0.5 mm thick ribbon which was then treated thermally at  $150^\circ\text{C}$ . Round tablets of  $3.2 \text{ cm}^2$  area were made from this strip, and 50 mg of active substance consisting of 85% oxide, 5% binder, 5% graphite and 5% acetylene black were distributed evenly on the surface of each tablet. After that, the tablets were pressed, heated at  $200^\circ\text{C}$ , pressed into the metallic case of the cell, and the whole cells were assembled by means of the common technological operations. The thickness of the active layer thus obtained was  $3.8 \cdot 10^{-3} \text{ cm}$ , accuracy limits being  $\pm 10\text{--}15\%$ .

Charges and discharges of experimental cells were accomplished by the potentiostat PI-50.1.1, the cells' temperature being maintained with thermostat at  $25 \pm 0.2^\circ\text{C}$ .

## 4. Results and discussion

Fig. 1 shows the examples of galvanostatic potential–time curves. Both charge and discharge curves exhibit clearly tangible inflection points at the potential about 3.6 and 2.1 accordingly. The times corresponding to these points should be attributed, evidently, to the end of the processes ( $\tau$  in Eqs. (6)–(12)).

The dependencies of capacity upon current density were obtained in two different ways. First, the charge current varied from cycle to cycle, and discharge current was small and constant (1 mA) in each cycle. Second, oppositely, the charge current was constant (1 mA) and the discharge current varied. Although both methods gave very close results, it was established, that the second allows for much wider range of currents to investigate. The fact is that above  $1.8 \text{ mA/cm}^2$ , the cells become irreversibly damaged, apparently, due to the growth of Li dendrites through the separator.

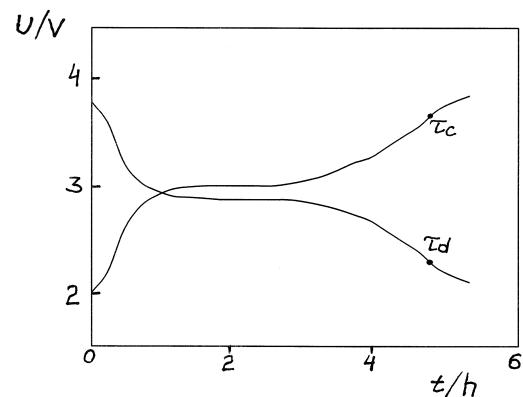


Fig. 1. Typical charge (1) and discharge (2) curves of rechargeable positive electrode based on tetragonal  $0.05 \text{ Li}_2\text{O} \cdot \text{MnO}_2$  oxide [5]. Operating current 1 mA, surface area  $3.2 \text{ cm}^2$ , total amount of the active substance 42.5 mg. The inflection points on charge ( $\tau_c$ ) and discharge ( $\tau_d$ ) curves correspond to the transition times of Eq. (10) or Eq. (12).

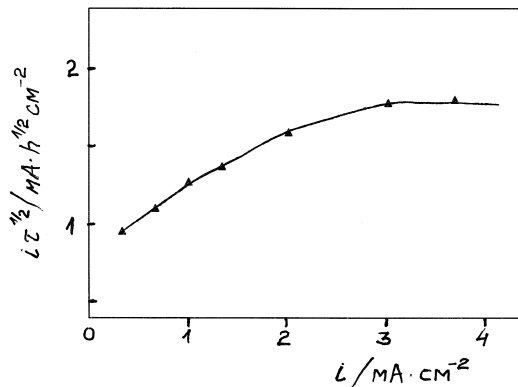


Fig. 2. The data of charge/discharge experiments represented in terms of Eq. (10).

Figs. 2 and 3 show the galvanostatic dependencies in the coordinates of Eqs. (10) and (12). The diffusion coefficient calculated by Eq. (12) from the slope of the linear part (Fig. 3) is equal to  $4.6 \cdot 10^{-8} \text{ cm}^2/\text{s}$ . By extrapolation of the line (Fig. 3) to  $i = 0$ , one can obtain the theoretical value of capacity per unit surface of the electrode  $Q_s = l \cdot F \cdot C_0$  (in  $\text{C}/\text{cm}^2$  or  $\text{mA h}/\text{cm}^2$ ) and the total concentration of active sites for Li,  $C_0$  ( $\text{mol}/\text{cm}^3$ ), which is a characteristic physicochemical property of the material. For the composition  $0.025 \cdot \text{Li}_2\text{O} \cdot \text{MnO}_2$ , to which the dependencies of Figs. 2 and 3 correspond, we obtain  $C_0 = 0.015 \text{ mol}/\text{cm}^3$ . Considering density and molecular weight, this gives the content of active vacancies per 1 Mn equal to 0.04.

The dependency shown in Fig. 2 contains the linear part at high current densities. The diffusion coefficient calculated from this value by Eq. (10) is equal to  $5.8 \cdot 10^{-8} \text{ cm}^2/\text{s}$ . Evidently, this value is in good agreement with the above obtained by Eq. (12) from the data at small current, considering the mathematical simplifications (see Appendix A), the assumption of the independence of  $D$  on the degree of charge, and possible error in the determination of the thickness of the active layer.

It follows from the presented model that an efficiency of a galvanostatic charge/discharge, i.e., the ratio of the

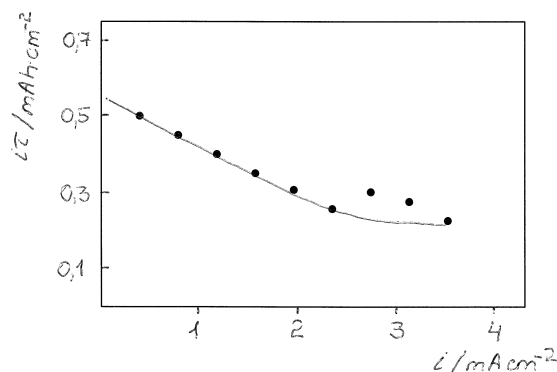


Fig. 3. The data of Fig. 2 as a function of  $i\tau(i)$  (Eq. (12)). The theoretical capacity and diffusion coefficient are calculated from the intersection of vertical axis and the slope of the linear part.

real achieved capacity to the theoretical value, decreases with current increase. From Eq. (12), one can derive the relation between charge current and prescribed efficiency  $\eta = Q/Q_m$ :

$$i_c = \frac{3 \cdot D \cdot Q_m (1 - \eta)}{l}, \quad (13)$$

where  $Q_m = F \cdot C_0$ , is the theoretical specific capacity of the material. Then, one of the most important service parameters, full charge time, is calculated as follows:

$$\tau_c = \eta \cdot l \cdot Q_m / i_c = \frac{l^2}{3D} \cdot \frac{\eta}{1 - \eta}. \quad (14)$$

In particular, for 1 mm thick rechargeable cathode based on  $\text{Li}_2\text{O}-\text{MnO}_2$  oxide [5], theoretical capacity is  $\sim 100 \text{ mA h/g}$  ( $F \cdot C_0 = 0.4 \text{ C}/\text{cm}^3$ ). Suppose the desired efficiency is  $\eta = 0.9$ , we obtain charge current  $i_c = 0.025 \text{ mA}/\text{cm}^2$  and time  $\tau_c = 180 \text{ h}$ . Reducing the demands to, e.g.,  $\eta = 0.8$ , we could increase the charge current to  $i_c = 0.05 \text{ mA}/\text{cm}^2$  and decrease the time to  $\tau_c = 80 \text{ h}$ .

## 5. Conclusions

As follows undoubtedly from the above results, not only the reversible capacity, but also the diffusion coefficient of  $\text{Li}^+$  ions, are of great importance for the development of commercial rechargeable lithium batteries. Some methods exist to estimate this value. The most common of them involves the calculation of  $D$  from the easily measurable electric conductivity [6]. This approach is unreliable for two reasons: (1) the Nernst–Einstein's equation should be used which is rather rough approximation; (2) strictly speaking, one must know not a total conductivity, but only ionic part of it, which, for many solids, is much less than electronic part and thus, is difficult to be measured. Among other methods, the calculation of  $D$  from potential decay curves after the current being switched off should be mentioned [7]; both theoretical capacity and degree of charge of the electrode must be known for the calculations, what is evidently the disadvantage. We believe that the method presented here, which permits the simultaneous determination of both maximum capacity and diffusion coefficient, will be useful in the researches and developments in the field of rechargeable lithium batteries.

## Appendix A

It is convenient to rewrite Eqs. (2)–(5) in the dimensionless form:

$$\frac{\partial Y}{\partial T} = \frac{\partial^2 Y}{\partial X^2}; \quad (1a)$$

$$T = 0; Y = 1; \quad (2a)$$

$$\left. \frac{\partial Y}{\partial X} \right|_{X=0} = J \quad (3a)$$

$$\int_0^1 Y dX = 1 - J \cdot T. \quad (4a)$$

The dimensionless variables  $X$ ,  $Y$ ,  $T$  and parameter  $J$  (dimensionless current) are defined here as:

$$X = \frac{x}{l}; \quad (5a)$$

$$Y = \frac{C}{C_0}; \quad (6a)$$

$$T = \frac{D \cdot t}{l^2} \quad (7a)$$

and

$$J = \frac{i \cdot l^2}{F \cdot D \cdot C_0} \quad (8a)$$

After Laplace's transform, we obtain the ordinary differential equation

$$\frac{d^2 F(S, X)}{dX^2} = S \cdot F(S, X) - 1 \quad (9a)$$

with transformed boundary conditions

$$\left. \frac{dF}{dX} \right|_{X=0} = \frac{J}{S} \quad (10a)$$

and

$$\int_0^1 F dX = \frac{1}{S} - \frac{J}{S^2} \quad (11a)$$

We are interested in the solution at  $X = 0$ . It is as follows:

$$F_0 = \frac{1}{S} - \frac{J}{S\sqrt{S}} \coth\sqrt{S}, \quad (12a)$$

where

$$\coth\sqrt{S} = \frac{e^{\sqrt{S}} + e^{-\sqrt{S}}}{e^{\sqrt{S}} - e^{-\sqrt{S}}} \quad (13a)$$

is a hyperbolic cotangent.

The reverse transform of Eq. (12a) is highly complicated. That is why we shall use, for small  $S$  (or large  $T$ ), the approximate formula for hyperbolic cotangents:

$$\coth z \approx \frac{1}{z} + \frac{z}{3}. \quad (14a)$$

Then

$$F_0 = \frac{1}{S} - \frac{J}{S^2} - \frac{J}{3S}, \quad (15a)$$

which corresponds to

$$Y_0 = 1 - \frac{J}{3} - J \cdot T. \quad (16a)$$

Taking  $Y_0 = 0$  at the end of the process, and using again the natural variables, we obtain Eq. (12).

For large  $S$  (small  $T$ ), we can use an approximation  $\sqrt{S} = 1$ . Then

$$F_0 = \frac{1}{S} - \frac{J}{S \cdot \sqrt{S}}, \quad (17a)$$

the reverse transform is equal to

$$Y_0 = 1 - \frac{2}{\sqrt{\pi}} \cdot J \cdot \sqrt{T}. \quad (18a)$$

Once again, taking  $Y_0 = 0$  and going over natural variables, we obtain Eq. (9) or Eq. (10).

## References

- [1] T. Nagaura, Prog. Battery Mater. 10 (1991) 209.
- [2] T. Ozuku, A. Ueda, J. Electrochem. Soc. 141 (1994) 2972.
- [3] J.B. Bates, D. Lubben, N.J. Dudney, F.X. Hart, J. Electrochem. Soc. 9 (1995) 149.
- [4] M.M. Tharckeray, Proc. WRS Symposium 135 (1989) 585.
- [5] A.A. Andriiko, L.I. Nyrkova, N.A. Chmilenko, P.V. Rudenok, Ye.V. Kuz'minskii, Solid State Ionics 86–88 (1996) 805–809.
- [6] R.A. Huggins, Phenomenology of ionic transport in solid-state battery materials, Solid State Batteries, Proc. NATO Adv. Study, 2–14 September 1984, pp. 5–16.
- [7] V.D. Prisiazhny, D.A. Tkalenko, N.A. Chmilenko, Doklady NAN Ukrainy 6 (1995) 104.